

Towards a better understanding on agglomeration mechanisms and thermodynamic properties of TiO₂ nanoparticles interacting with natural organic matter

Frédéric Loosli^a, Leticia Vitorazi^b, Jean-François Berret^b and Serge Stoll^{a,*}

Affiliations:

^a Group of Environmental Physical Chemistry, University of Geneva, F.-A. Forel Institute Section des Sciences de la Terre et de l'Environnement, 10 route de Suisse, 1290 Versoix, Switzerland

^b Laboratoire Matière et Systèmes Complexes, UMR 7057 Université Paris-Diderot/CNRS, Bâtiment Condorcet, 10 rue Alice Domon et Léonie Duquet, F-75205 Paris cedex 13, France

*Corresponding Author and Address:

Serge Stoll^{*}: Group of Environmental Physical Chemistry, University of Geneva, F.-A. Forel Institute, Section des Sciences de la Terre et de l'Environnement, 10 route de Suisse, 1290 Versoix, Switzerland

Phone: + 41 22 379 0333; Fax: + 41 22 379 0302

email: serge.stoll@unige.ch

Abstract

Interaction between engineered nanoparticles and natural organic matter is investigated by measuring the exchanged heat during binding process with isothermal titration calorimetry. TiO₂ anatase nanoparticles and alginate are used as engineered nanoparticles and natural organic matter to get an insight into the thermodynamic association properties and mechanisms of adsorption and agglomeration. Changes of enthalpy, entropy and total free energy, reaction stoichiometry and affinity binding constant are determined or calculated at a pH value where the TiO₂ nanoparticles surface charge is positive and the alginate exhibits a negative structural charge. Our results indicate that strong TiO₂-alginate interactions are essentially entropy driven and enthalpically favorable with exothermic binding reactions. The reaction stoichiometry and entropy gain are also found dependent on the mixing order. Finally correlation is established between the binding enthalpy, the reaction stoichiometry and the zeta potential values determined by electrophoretic mobility measurements. From these results two types of agglomeration mechanisms are proposed depending on the mixing order. Addition of alginate in TiO₂ dispersions is found to form agglomerates due to polymer bridging whereas addition of TiO₂ in alginate promotes a more individually coating of the nanoparticles.

Keywords: TiO₂ nanoparticles, alginate, natural organic matter, isothermal titration calorimetry, metal oxide stability, aquatic systems

1. Introduction

Nanoparticles are produced in increasing quantities due to their unique surface properties (Auffan et al. 2009, Gottschalk et al. 2009) and are used in many domains and applications (Chen and Mao 2007, Lu et al. 2007, Luo et al. 2006). A non negligible amount of these engineered nanoparticles (ENPs) is thus entering aquatic systems as individual or agglomerated nanoparticles through industrial discharges, surface runoff from soils or from wastewater treatment effluent (Batley et al. 2013, Seitz et al. 2012). Once in aquatic environments, interactions with natural compounds will modify their stability, fate, bioavailability and toxic effects towards living organisms (Christian et al. 2008, Handy et al. 2008, Klaine et al. 2008, von Moos and Slaveykova 2014).

Among ENPs, TiO₂ nanoparticles are produced in high tonnage (Piccinno et al. 2012) and are present in many customer products such as food, cosmetic and painting industries (Chen and Mao 2007, Cozzoli et al. 2003, Gratzel 2004, Jimin et al. 2010, Khan and Dhayal 2008, Mahltig et al. 2005, Weir et al. 2012, Wongkalasin et al. 2011, Zhang and Sun 2004). TiO₂ ENPs production exceeds tons per year (Hendren et al. 2011, Piccinno et al. 2012, Schmid and Riediker 2008) and the expected concentration present in aquatic systems is in the ng L⁻¹ to µg L⁻¹ range (Batley et al. 2013, Gottschalk et al. 2009, Sani-Kast et al. 2015). Therefore TiO₂ is often considered to study the possible transformations of nanoparticles in aquatic systems. Most of the studies on TiO₂ ENPs transformation processes in presence of natural organic matter (NOM) demonstrate that humic substances and non humic substances such as extracellular polymeric substances are found to deeply modify the TiO₂ stability (Belen Romanello and Fidalgo de Cortalezzi 2013, Chae et al. 2012, Domingos et al. 2009, Erhayem and Sohn 2014, Gallego-Urrea et al. 2014, Shen et al. 2015, Zhang et al. 2013). Indeed recent findings considering the effect of NOM have shown that electrostatic repulsions and steric interactions between NOM molecules adsorbed onto the ENPs surface enhance the stability and thus the ENPs dispersion state (Hyung et al. 2007, Liu et al. 2010, Loosli et al. 2013, Louie et al. 2013, Palomino and Stoll 2013, Zhang et al. 2009). Moreover NOM complexation with ENPs is also found to induce the partial redispersion of already formed ENP agglomerates (Baalousha 2009, Loosli et al. 2014, Mohd Omar et al. 2014). All these studies are investigating the ENPs surface charge modification and give a special interest to the ENPs state of dispersion (resulting size, charge and stability of the ENPs) in presence of NOM. In the present study, a particular concern is given to the quantification of thermodynamic interaction parameters using isothermal titration calorimetry (ITC) for the investigation of interactions between anatase TiO₂ ENPs and alginate, an extracellular polymeric substance model (Bernhardt et al. 1985, Gregor et al. 1996). Indeed polysaccharides represent 10-30% of the NOM in lakes (Buffle et al. 1998, Wilkinson et al. 1999, Wilkinson et al. 1997) whereas in marine environment polysaccharide content may be as high as 50% of the dissolved organic carbon (Engel et al. 2004, Wells 1998). Alginate is a naturally occurring polysaccharide and is found in aquatic environments (Gombotz and Wee 1998). It is produced by brown algae species but also by some bacteria (Gombotz and Wee 1998, Saude et al. 2002). Alginate is a negatively charged linear block copolymer composing of 1→4 linked β-D-mannuronic acid and its C-5 epimer α-L-guluronic acid. Alginate is also used as a thickener

agent in food industry and as drug carrier in biomedicine (Helgerud 2009, Lee and Mooney 2012). ITC is a universal method which is suitable to follow the energies of association reactions. Indeed important parameters that are global properties of the systems such as the change of enthalpy ΔH , the change of entropy ΔS and the change of the total free energy ΔG that occur during the binding processes can be extracted. ITC measurements also provide information on the interaction affinity by determination of the affinity binding constant K_b and the interaction reaction stoichiometry. All these parameters are accessible through a single experiment. This method has been applied to a wide range of chemical and biochemical binding interactions and was especially used for protein-substrate interactions, structure-based drug design and supramolecular polymers self-associations (Arnaud and Bouteiller 2004, Brinatti et al. 2014, Cedervall et al. 2007, Chiappisi et al. 2013, Doyle 1997, Jelesarov and Bosshard 1999, Kamiya et al. 1996, Kim et al. 2010, Ladbury 2001, Matulis et al. 2002, Vitorazi et al. 2014). Humic acid coverage on arsenic was shown to slightly reduce the binding interaction and the rate constant between arsenic-coated and ferrihydrite-kaolinite mixtures (Martin et al. 2009). Sheng et al. investigated the binding properties of copper ions with extracellular polymeric substances and showed that the process was mainly driven by entropy (Sheng et al. 2013). Another study on alginate-sodium dodecyl sulfate interaction shown that aggregation was due to hydrophobic interactions (Yang et al. 2008). Thermodynamic adsorption profile at a solvated organic-inorganic interface was done and gold ENPs interaction with carboxylic acid-terminated alkanethiols was found exothermic and enthalpy driven (Joshi et al. 2004, Ravi et al. 2013).

The present work is dealing with a novel approach that has a high potential to contribute to a better understanding of the behavior of ENPs in the presence of NOM. A detailed description is achieved on the complex interaction phenomena which occur between ENPs and NOM by determining key thermodynamic parameters and their link with ENPs surface charge properties to understand agglomeration mechanisms. Such quantitative information is often missing when ENP interactions with aquagenic compounds have to be investigated.

2. Materials and methods

2.1. Materials

TiO₂ engineered nanoparticles were obtained from Nanostructured & Amorphous Material Inc (Houston, TX, USA) as a 15% wt suspension of 15 nm anatase nanoparticles in water (Loosli et al. 2013). This stock solution was then, after homogenization, diluted by adding Milli Q water (Millipore, Zoug, ZG, Switzerland, with R >18 M Ω .cm, T.O.C. <2 ppb) to reach a final 5 g L⁻¹ TiO₂ mass concentration. For sodium alginate (A2158, Sigma Aldrich, Buchs, SG, Switzerland) a 10 mM solution in term of charge concentration was prepared by dissolving the low viscosity biopolymer in MilliQ water and by stirring it overnight. NaOH and HCl (1 M, Titrisol[®], Merck, Zoug, ZG, Switzerland) were used after dilution to adjust the dispersions and solutions at pH 3.1 and 11.0. The compounds were dialyzed simultaneously into the same water buffer using separate 12-14 kDa cutoff dialysis membranes (Spectrum Laboratories, Inc., Rancho Dominguez, CA, USA) to minimize the change of enthalpy (ΔH)

from dilution process during titration. The solvent from the dialysis was used to dilute the TiO₂ and alginate suspensions to experimental concentrations (from 0.1 to 1.4 g L⁻¹ for TiO₂ and from 0.05 to 2.5 mM for alginate). Finally, prior utilization they were filtered through a 0.45 μm cellulose acetate filter (VWR, Nyon, VD, Switzerland) to remove possible presence of laboratory air dust. No loss of TiO₂ and alginate was observed during the filtration process.

2.2. Isothermal titration calorimetry measurement

The heat exchange between TiO₂ ENPs and alginate was determined using a VP-ITC calorimeter (MicroCal Inc., Northampton, MA, USA) with a sample cell volume equal to 1.4643 mL. The working temperature was set to 298.15 K and, after a preliminary 2 μL ligand (L) injection, 28 injections of 10 μL of ligand into the sample cell containing 1.4643 mL (which is equal to the cell volume) of the macromolecule (M) were realized with an injection duration of 20 seconds and a 210 seconds delay between each successive injection. The agitation speed was set to 307 rpm. Equation (Eq. (1)) to fit the data representing the heat of exchange (dQ/dn_L) during the association process as a function of the molar charge ratio (Z = [L]/[M], where [L] and [M] are the ligand and macromolecule molar charge concentration) was derived from the Multiple Non-Interacting Sites (MNIS) model where binding sites are considered to be independent (Courtois and Berret 2010).

$$\frac{dQ}{dn_L}(Z) = \frac{1}{2} \Delta H_b \left[1 + \left(1 - \frac{[L]}{n[M]} - \frac{1}{n K_b [M]} \right) \left(\left(1 + \frac{[L]}{n[M]} + \frac{1}{n K_b [M]} \right)^2 - \frac{4[L]}{n[M]} \right)^{-\frac{1}{2}} \right] \quad (1)$$

In Eq. (1) the fitting parameters ΔH_b in kJ mol⁻¹, K_b in M⁻¹ and n represent the binding enthalpy, binding constant and reaction stoichiometry respectively. The system total free energy, ΔG in kJ mol⁻¹, and entropy, ΔS in kJ K⁻¹ mol⁻¹, are calculated from the fitting parameters (K_b and ΔH_b values) with ΔG = -RTlnK_b and ΔS = (ΔH-ΔG)/T. The ligand and macromolecule charge numbers for the *i*th-injection are equal to:

$$L_i = L_{i-1} + V_i \cdot [L]_m \cdot N_A \quad \text{and} \quad M = [M]_m \cdot V_{cell} \cdot N_A \quad (2)$$

$$\text{with } [TiO_2]_m = [TiO_2]_M \cdot S_A \cdot \sigma_{TiO_2} \cdot 10^{18} \div N_A \quad \text{and} \quad (3)$$

$$[Alginate]_m = [Alginate]_M \div MW(\text{monomer}) \cdot \alpha \quad (4)$$

In Eq. (2), V_i and V_{cell} represent the volume of ligand injected and the cell volume respectively, [L or M]_m correspond to the mol of charge of ligand or macromolecule per unit of volume and N_A to the Avogadro constant. The concentration in term of mol of charge per unit of volume for TiO₂ and alginate are expressed in Eq. (3) and (4) respectively. In Eq. (3), [TiO₂]_M represent the TiO₂ mass concentration, S_A the ENPs specific surface area and σ_{TiO₂} the TiO₂ hydroxyl sites density. In Eq. (4) [Alginate]_M represents the alginate mass concentration and α the degree of ionization.

TiO₂ charge concentrations were calculated based on manufacturer data of the primary TiO₂ diameter (equal to 15 nm and in good agreement with the mode value of the number size distribution determined by dynamic light scattering, Fig. S2b) to calculate S_A and on the other

hand on a previous study to obtain σ_{TiO_2} (Kominami et al. 2000). A S_A and σ_{TiO_2} equal to $100 \text{ m}^2 \text{ g}^{-1}$ and 5 sites nm^{-2} respectively were used to determine the TiO_2 charge concentration. The factor of conversion between the mass and charge concentration was thus set so that a 1 g L^{-1} TiO_2 dispersion corresponds to a 0.83 mM charge concentration. The degree of ionization of alginate was set equal to 1 (completely deprotonated) due to the net polymer carboxylic acid moieties pK_a decrease in presence of strongly oppositely charged particles (Carnal and Stoll 2011).

Furthermore the mixing order of the two compounds was investigated to better understand the TiO_2 -alginate and alginate- TiO_2 interactions and the agglomeration process as illustrated in Fig. 1. In a first set of experiments (type I) alginate was playing the role of ligand and was added to the TiO_2 dispersion. In the second set of experiments realized (type II) TiO_2 ENPs (L) were added to alginate (M).

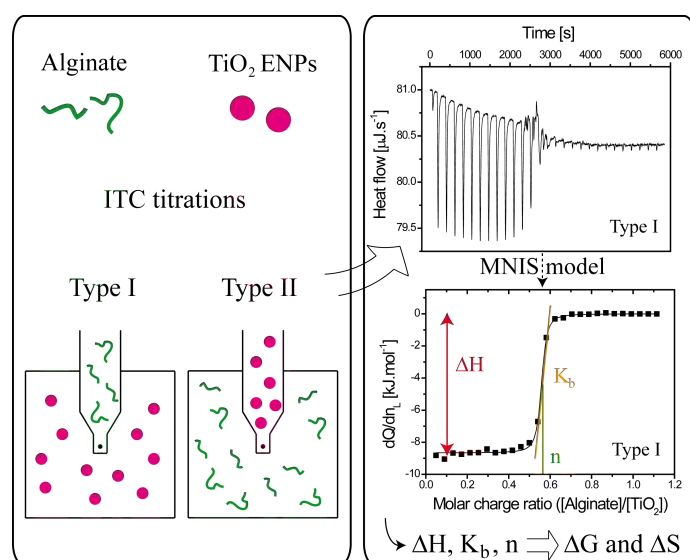


Fig. 1 - ITC type I (alginate in TiO_2 dispersion) and type II (TiO_2 in alginate) titrations. ITC measurements give the heat flow for each of the 28 injections and after fitting the integrated data with the multiple non-interacting sites (MNIS) model the enthalpy of exchange ΔH , the binding constant K_b and the reaction stoichiometry n are determined. It permits the calculation of the entropy ΔS and total free energy ΔG for TiO_2 -alginate interaction.

Experiments were realized at $\text{pH } 3.1$ (and at $\text{pH } 11.0$ for negative controls) without addition of electrolyte. Such a pH value was utilized to address the interaction between isolated, dispersed ENPs and alginate. It is important to note that results presented here remains valid as long as $\text{pH} < \text{pH}_{\text{PCN},\text{TiO}_2}$. Moreover this pH corresponds to the commercial dispersion pH (after dilution to a 5 g L^{-1} concentration) and was chosen to avoid any pH surface charge modification effects. The domain of concentration investigated was from 0.5 mM alginate in 0.1 g L^{-1} TiO_2 to 2.5 mM alginate in 0.5 g L^{-1} TiO_2 for Type I experiments and from 1 g L^{-1} TiO_2 in 0.05 mM alginate to 5 g L^{-1} TiO_2 in 0.25 mM alginate for Type II experiments. Such TiO_2 concentration are higher than the expected environmental concentration, which are in the ng to $\mu\text{g L}^{-1}$ range (Batley et al. 2013, Gottschalk et al. 2009, Sani-Kast et al. 2015), because

of the importance to obtain an optimum signal with the calorimeter. Also it should be noted that concentrations could be significantly higher than the expected environmental concentration in case of local pollution events.

2.3. Zeta potential and size distribution measurements

Zeta (ζ) potential values and z-average hydrodynamic diameters of TiO_2 dispersion and alginate solution as a function of pH as well as TiO_2 in presence of alginate (for Type I and II titrations) as a function of charge ratio were determined by measuring the particles velocity using laser doppler velocimetry with phase analysis light scattering (M3-PALS) and diffusion coefficient using dynamic light scattering (DLS) (Zetasizer Nano ZS instrument, Malvern Instruments, Worcestershire, UK). The instrument was operating at 298.15 K with a 4 mW He-Ne laser working at 633 nm and the detection angle for DLS measurement was 173° (back scattering). For ζ potential values determination the Smoluchowski approximation model was applied according to the formation of large agglomerates (Baalousha 2009). All polydispersity indexes were found below 0.6.

3. Results and discussion

To determine the binding properties between TiO_2 ENPs and alginate, ITC experiments were realized at $\text{pH} < \text{pH}_{\text{PCN},\text{TiO}_2}$ where strong electrostatic interactions occur between the negatively charged alginate and positively charged TiO_2 ENPs. As shown in Fig. 2, in which the ζ potential values of TiO_2 and alginate are represented as a function of pH, at pH 3.1 (large gray vertical line) the ENPs exhibit a positive surface charge (ζ potential = $+40.9 \pm 1.4$ mV (mean \pm standard deviation on mean of triplicates)) and the biopolymer structural charge is negative with a ζ potential value found equal to -13.0 ± 0.1 mV. At $\text{pH} < \text{pH}_{\text{PCN},\text{TiO}_2}$ the TiO_2 ENPs are dispersed with a z-average diameter equal to 47 ± 1 nm (Figs. S1 and S2 in Supporting information) and alginate z-average diameter is equal to 178 ± 21 nm (Figs. S3 and S4).

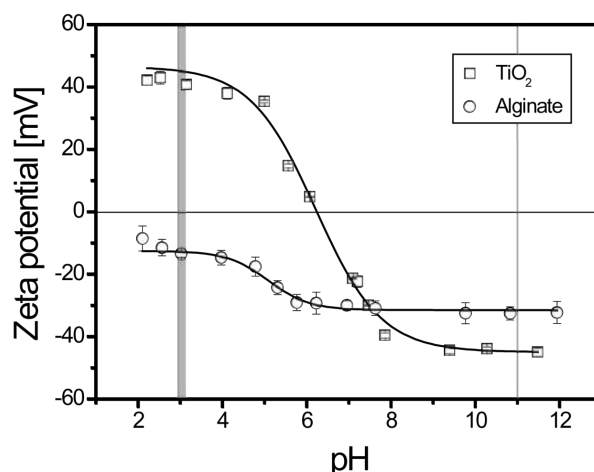


Fig. 2 - Zeta potential values of TiO_2 (open squares) and alginate (open circles) as a function of pH. TiO_2 isoelectric point is found here equal to 6.2 ± 0.1 whereas alginate exhibit a negative structural charge in the full pH range. At pH 3.1 TiO_2 and alginate have ζ potential values equal to $+40.9 \pm 1.4$ mV and -13.0 ± 0.1 mV respectively (large gray vertical line). At pH 11.0 both compounds are negatively charged (narrow gray vertical line). $[\text{TiO}_2] = 50 \text{ mg L}^{-1}$, $[\text{Alginate}] = 100 \text{ mg L}^{-1}$ and $[\text{NaCl}] = 0.001 \text{ M}$.

3.1. Determination of TiO₂-Alginate thermodynamic binding parameters by ITC

Titration of TiO₂ dispersion with alginate (Type I) When alginate is added to TiO₂ ENPs strong interactions are observed as shown in Fig. 3a which represents a thermogram of the heat of exchange as a function of time for a 100 mg L⁻¹ TiO₂ dispersion titrated by a 0.5 mM alginate charge concentration. Generally when adding alginate to the TiO₂ dispersion the instrument responds so as to compensate the binding reaction exchange energy to maintain a small difference of temperature between the reference cell and the "reaction" cell constant. Both cells are isolated in an adiabatic jacket. The heat compensation is recorded and in the present case "negative" peaks reveal an exothermic process. Each peak corresponds to a consecutive alginate addition. In the thermogram the first response (first peak) is of lower intensity than the following owing to the smaller alginate volume injected (2 μL instead of the 10 μL "normal" injection volume). For the next ten injections the peak amplitudes are constant. It means that the number of TiO₂ free sites available for random alginate adsorption is high enough to undergo adsorption of a maximum and identical alginate amount. Then the peak intensity rapidly decreases as less positively TiO₂ sites are available and finally only low heat exchange corresponding to dilution effect is observed for the last injections due to sites saturation (exchange energy identical to alginate titration in water at pH 3.1, as shown in Fig. S5, with dilution giving rise to low exothermic interaction).

From the data presented in Fig. 3a, the variation of the exchange energy as a function of alginate over TiO₂ charge ratio ($Z = [\text{Alginate}]/[\text{TiO}_2]$) is plotted in Fig. 3b. The values of interaction heat of exchange (dQ/dn_L) for each injection are equal to the corresponding peak area integration from the real-time thermogram. For the 100 mg L⁻¹ TiO₂ titration with 0.5 mM alginate the binding enthalpy is found equal to -8.7 kJ mol⁻¹ which indicates an exothermic interaction process. K_b is equal to $3.5 \times 10^7 \text{ M}^{-1}$ which points out a high binding affinity between TiO₂ and alginate in this electrostatic scenario (positively charged TiO₂ ENPs in the presence of negatively charged alginate). The reaction stoichiometry is found equal to 0.56. All these fitting parameters (derived from Eq. (1)) allow the calculation of the free energy ΔG and entropy ΔS changes during the interaction process. These energy changes are equal to $-4.3 \times 10^4 \text{ kJ mol}^{-1}$ and $+115.3 \text{ J mol}^{-1} \text{ K}^{-1}$ respectively. Two other experiments with different concentrations but with the same $[L]/[M]$ ratio have been done to evaluate the effect of relative concentration on binding processes. The real-time thermograms and respective integrated heat data fitted with the MNIS model for these experiments are represented in Figs. S6 and S7 and all the fitting and calculated parameters derived from the type I titrations are listed in Table 1.

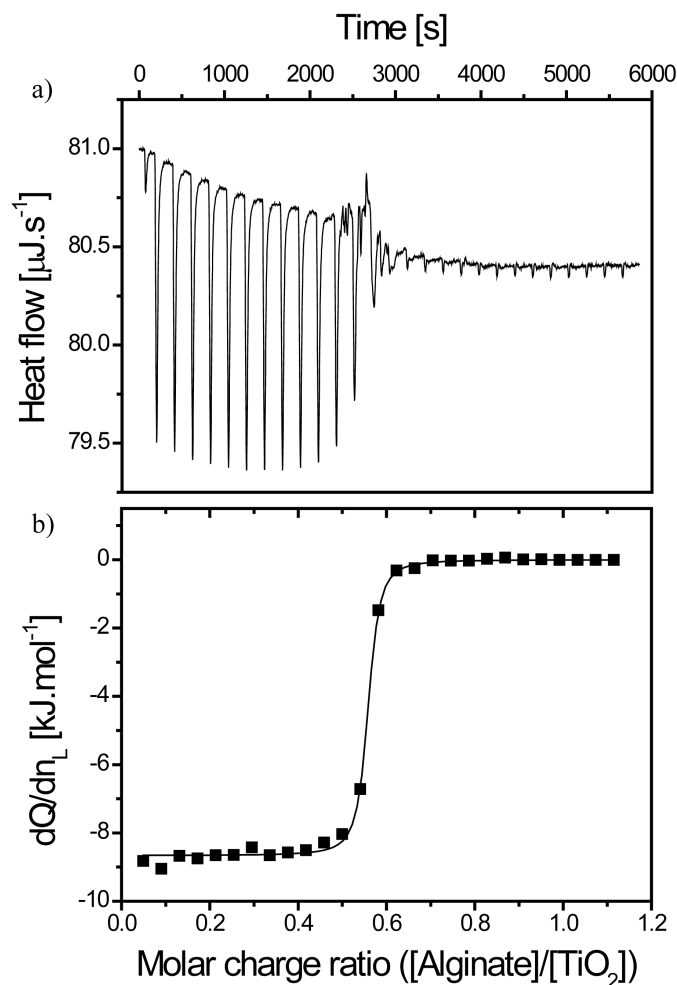


Fig. 3 - a) Real-time thermogram for TiO_2 0.1 g L^{-1} titration with alginate 0.5 mM at $\text{pH} < \text{pH}_{\text{PCN},\text{TiO}_2}$ and at 298.15 K . The heat flow refers to the thermal compensation of the calorimeter to keep the sample at a constant temperature. Here negative peaks indicate an exothermic reaction. After about fifteen injections sites saturation occurs and only dilution effect is observed (small negative peaks). b) The respective integrated heat data (dQ/dn_L) as a function of molar charge ratio ($[\text{Alginate}]/[\text{TiO}_2]$) is fitted with the multiple non-interacting sites (MNIS) model. The binding enthalpy, the binding constant and the reaction stoichiometry where found here equal to -8.7 kJ mol^{-1} , $3.5 \times 10^7 \text{ M}^{-1}$ and 0.56 , respectively.

Table 1: Fitting parameters ΔH_b , K_b and n from ITC analysis of the integrated heats with MNIS model and calculated ΔG and ΔS from K_b and ΔH_b values. The formation of complexes between TiO_2 ENPs and alginate is found spontaneous, mainly driven by entropic effects and enthalpically favorable.

Alginate in TiO_2	ΔH_b [kJ mol^{-1}]	K_b [M^{-1}]	n	ΔG [kJ mol^{-1}]	ΔS [$\text{J K}^{-1} \text{ mol}^{-1}$]
0.5 mM in 0.1 g L^{-1}	-8.7	3.5×10^7	0.56	-43.0	115.3
0.7 mM in 0.14 g L^{-1}	-9.0	2.4×10^7	0.56	-42.2	111.3
2.5 mM in 0.5 g L^{-1}	-8.7	1.3×10^7	0.61	-40.6	107.2

Alginate interaction with TiO₂ ENPs is found to be a spontaneous process with high values of Gibbs free adsorption energy ($\Delta G < -40 \text{ kJ mol}^{-1}$). The binding enthalpy is favorable to the formation of complexes ($\Delta H_b < 0$) and found independent on the compounds concentration. The main interaction driving process is due to an important gain in entropy ($-T\Delta S < \Delta H_b$) with T ΔS value of about $+30 \text{ kJ mol}^{-1}$ in our experimental conditions. The binding constant is found to decrease when increasing concentration as $K_b \sim c^{-2}$. It implicates the decrease of the calculated Gibbs free energy and entropy (Courtois and Berret 2010) as the binding enthalpy change is constant and independent on concentration ($-8.8 \pm 0.2 \text{ kJ mol}^{-1}$). The charge stoichiometry was found constant with $n = 0.58 \pm 0.04$.

Titration of alginate with TiO₂ (Type II) The ITC thermogram and the respective integrated heat data for a TiO₂ 1 g L^{-1} and 0.05 mM alginate reaction are shown in Fig. 4. The interaction is also found exothermic and for a charge ratio around $Z = 1$ no further interaction between TiO₂ and alginate occurs and only dilution effect is observed (same exchange heat than in Fig. S8 for TiO₂ titration in water). In Table 2 thermodynamic parameters are listed for experiments at different concentrations (Figs. S9 and S10). The binding enthalpy is found independent of the concentration and equal to $-8.7 \pm 0.4 \text{ kJ mol}^{-1}$ and the complexation process is also driven by an important entropy gain.

Table 2: Fitting parameters ΔH_b , K_b and n from ITC analysis of the integrated heats with MNIS model and calculated ΔG and ΔS from K_b and ΔH_b values. The formation of complexes between TiO₂ ENPs and alginate is found spontaneous, mainly driven by entropic effects and enthalpically favorable.

TiO ₂ in Alginate	ΔH_b [kJ mol^{-1}]	K_b [M^{-1}]	n	ΔG [kJ mol^{-1}]	ΔS [$\text{J K}^{-1} \text{ mol}^{-1}$]
1 g L^{-1} in 0.05 mM	-8.2	1.6×10^7	0.82	-41.1	110.3
1.4 g L^{-1} in 0.07 mM	-9.0	1.4×10^7	0.96	-40.8	106.6
5 g L^{-1} in 0.25 mM	-8.8	7.9×10^6	0.93	-39.4	102.6

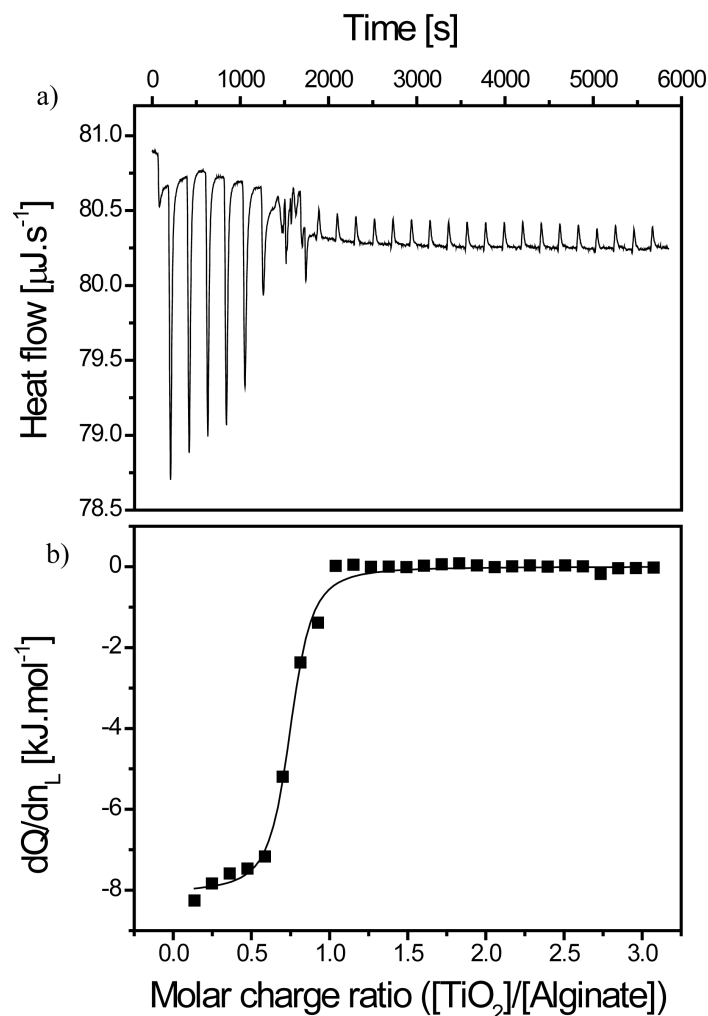


Fig. 4 - a) Real-time thermogram for alginate 0.05 mM titration with TiO_2 1 g L^{-1} at $\text{pH} < \text{pH}_{\text{PCN},\text{TiO}_2}$ and at 298.15 K. Negative peaks indicate an exothermic reaction and after about ten injections sites saturation occurs and only dilution effect is observed (small positive peaks). b) The respective integrated heat data as a function of TiO_2 over alginate molar charge ratio is fitted with the MNIS model. The binding enthalpy, the binding constant and the reaction stoichiometry are found here equal to -8.2 kJ mol^{-1} , $1.6 \times 10^7 \text{ M}^{-1}$ and 0.82, respectively.

When comparing the two titration types similar binding enthalpy value are observed. Both types of interaction are enthalpically favorable but mainly driven by entropic gain arising from the alginate and ENP counter-ions and water molecules release during adsorption processes. Similar total free energy changes were observed during the association process between ZnO NPs with lysozyme, as well as between proteins and amino acid functionalized gold NPs (Chakraborti et al. 2010, Chatterjee et al. 2010, De et al. 2007). However it should be noted here that the interaction process is mainly driven by an important gain of entropy whereas in the other studies (Chakraborti et al. 2010, Chatterjee et al. 2010) the strong interactions ($K_b = 0.9 \times 10^6 \text{ M}^{-1}$) were enthalpically favorable but entropically unfavorable due to conformational restriction of proteins. Reaction stoichiometry close to unity clearly indicates that the interaction is electrostatic. When working in conditions where electrostatic

interactions are favorable (positively charged ENPs and negatively charged polysaccharides) a stoichiometry close to unity in term of molar charge ratio denotes an electrostatic driven process for compounds in which charges are not sterically hindered (which is the case here for both TiO_2 and alginate) and where other functional groups (such as alcohol) are not playing main roles. Nevertheless the stoichiometry of the two titration types is different and explained by different mechanisms of interaction depending on the mixing order. For type I, when alginate is added to TiO_2 , the polysaccharide is prompt to facilitate bridging between the ENPs which restrict the access to positive TiO_2 charges due to conformational hindrance during bridging agglomeration process. Consequently the stoichiometry is smaller than unity ($n = 0.58 \pm 0.04$).

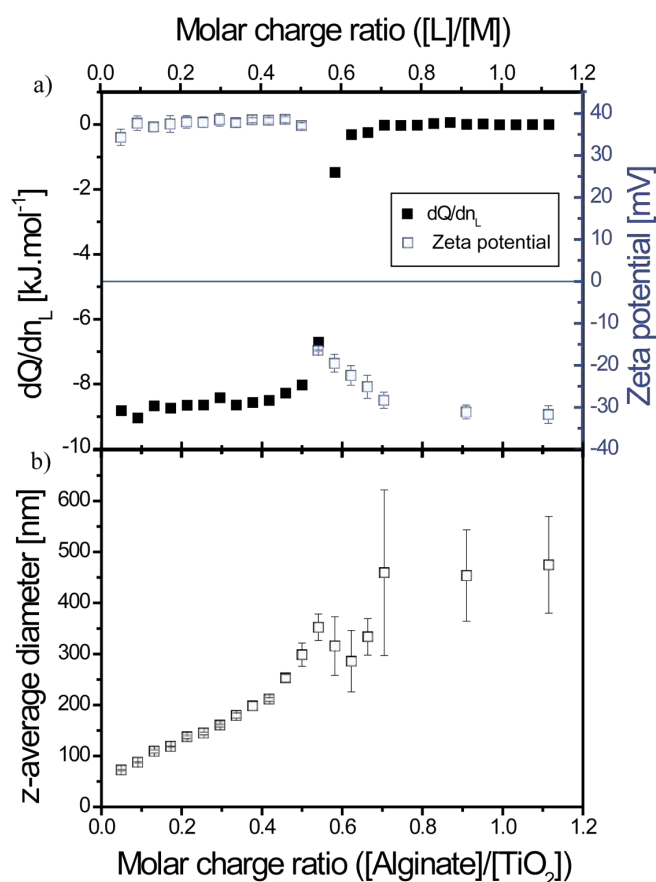


Fig. 5 - a) Integrated heat data and ζ potential values as a function of alginate over TiO_2 charge ratio for TiO_2 0.1 g L^{-1} titration with alginate 0.5 mM at $\text{pH} < \text{pH}_{\text{PCN},\text{TiO}_2}$. For a ratio up to 0.5, the binding enthalpy and the ζ potential values are constant and found equal to $-8.8 \pm 0.3 \text{ kJ mol}^{-1}$ and $+37.6 \pm 0.3 \text{ mV}$. Then charge inversion (ζ potential = $-16.4 \pm 0.2 \text{ mV}$) is observed for $Z = 0.54$ and for $Z > 0.70$ sites saturation occurs and no more interaction is observed. b) z-average diameter as a function of molar charge. Strong TiO_2 ENPs destabilization occurs for $Z > 0.5$ whereas, below this ratio, z-average diameter increase is linear indicating ENPs bridging.

For type II titration, when TiO_2 is added to alginate the ENPs are more closely individually coated and the charge stoichiometry is closer to the unity ($n = 0.90 \pm 0.07$). These different

mechanisms are related to the initial predominant compound concentration and physico-chemical properties in the reaction cell. The bridging mechanism in type I is favorable to higher entropy gain (ΔS columns in Tables 1 and 2). Indeed, in addition to entropy gain due to the polymer counter-ions and water molecules release, alginate is expected to be less collapsed onto the ENPs surface and thus lower conformational entropy loss is observed than in the type II titration. This conformational entropy gain is nevertheless negligible in comparison to the entropy gain due to counter-ions and water molecule release. Another similarity between the type I and type II titrations is the heat exchange signature on real-time thermogram for the injection just prior binding sites saturation which is the consequence of an important system physical change (as discussed below).

To ensure that electrostatic interactions are governing the complexation process a negative control was done at pH 11.0. At this pH both the TiO_2 and the alginate exhibit negative surface and structural charges (Fig. 2), respectively, and no interaction was observed due to electrostatic repulsions between the two compounds (Fig. S11).

3.2. Influence of TiO_2 -alginate complexes structural charge on binding heat of exchange

Determination of the ζ potential and hydrodynamic diameter values for the type I and ζ potential values for type II titrations are done here to evaluate charge modification during titration process and correlate it with the heat exchange values determined from ITC measurements. The time between each successive ligand addition was equal to 210 seconds similarly to the ITC titrations. Hydrodynamic diameters values for type II titration were not determined owing to the insufficient DLS signal until the 8th injection (sites saturation).

Type I titration: The binding enthalpy and ζ potential values as a function of molar charge ratio for type I titration, alginate 0.5 mM in TiO_2 0.1 g L⁻¹ at pH 3.1, are represented in Fig. 5. For an alginate over TiO_2 charge ratio up to 0.50, binding enthalpy per mol of injectant as well as the ζ potential are constant and equal to -8.8 ± 0.3 kJ mol⁻¹ and $+37.6 \pm 0.3$ mV respectively. High ζ potential values in this molar charge ratio domain indicates that TiO_2 surface coverage is far to be complete and enough TiO_2 positively charged binding sites are available for further alginate adsorption which is confirmed by constant and maximum interaction enthalpy values. Then for a ratio of 0.54 TiO_2 charge inversion is observed (ζ potential = -16.4 ± 0.2 mV) and the corresponding binding enthalpy is decreasing to -1.6 kJ mol⁻¹. For the three next alginate injections the ζ potential values and the binding enthalpy slightly decrease and, for a charge ratio greater than 0.70, sites saturation occurs and no interaction between alginate and TiO_2 is recorded, due to electrostatic repulsions and steric effects at high alginate concentration as shown by Lin et al. (Lin et al. 2012), with a corresponding ζ potential plateau value at -30.4 ± 1.8 mV. The z-average diameter of the TiO_2 ENPs as a function of the molar charge ratio Z is represented in Fig. 5b. Two domains in term of size variation are observed. In the first one, for a charge ratio below 0.5, the TiO_2 z-average diameter increases linearly when alginate is added. This is due to the alginate polymer bridging between the ENPs. Then a second domain is reached for further alginate addition

were stronger destabilization of TiO₂ is observed due to surface charge neutralization and inversion which result in particle precipitation.

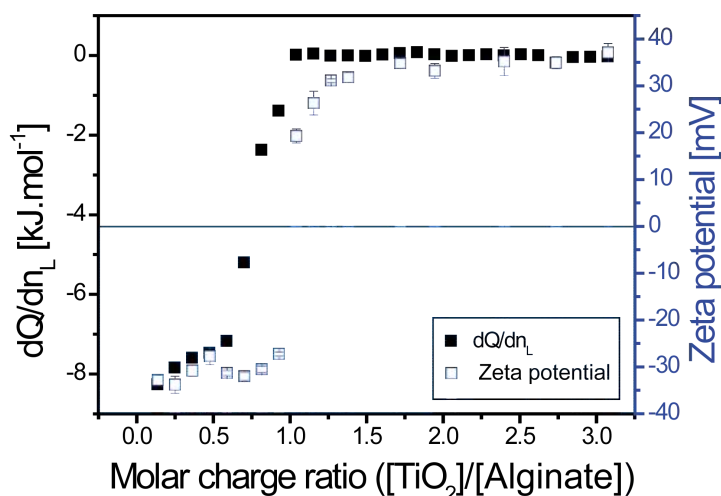


Fig. 6 - Integrated heat data and ζ potential values as a function of TiO₂ over alginate charge ratio for an alginate 0.05 mM titration with TiO₂ 1 g L⁻¹ at pH < pH_{PCN,TiO₂}. For a charge ratio equal to 1, charge inversion is observed (ζ potential = +19.3 ± 1.5 mV) and interactions are no longer occurring.

Type II titration: In Fig. 6 is presented the variation of ζ potential and binding enthalpy as a function of TiO₂ over alginate molar charge ratio for the titration of a 0.05 mM alginate solution with a 1 g L⁻¹ TiO₂ dispersion at pH < pH_{PCN,TiO₂}. Net decrease of TiO₂-alginate interaction takes place after six ENPs injections and, for a molar ratio equal to 1, charge inversion is observed with ζ potential values found equal to +19.3 ± 1.5 mV. Then by further increasing the TiO₂ concentration thermodynamic interactions are no longer observed.

A good agreement is found between the ζ potential and the interaction enthalpy values for both titration mode (type I and type II) as well as with the z-average diameter values for the type I titration. For the type I and II titrations TiO₂-alginate thermodynamic interactions are not occurring when charge inversion and sites saturation are observed (for $Z \geq 0.7$ and 1, respectively) due to electrostatic repulsions and steric effects between the TiO₂-alginate agglomerates and the titrant. Hence simple dilution effect is observed. The main difference between the two types of titration is the molar charge ratio needed to achieve charge inversion ($Z \approx 0.5$ for type I whereas $Z \approx 1$ for type II). When alginate is added to the TiO₂ dispersion, alginate is bridging the TiO₂ as shown by z-average diameter values increase for $Z \leq 0.5$ which confirms the bridging mechanism of agglomeration. Dynamic light scattering permits to assign the real-time thermogram signature occurring prior non-interaction domain to an important precipitation domain in agreement with z-average diameter and ζ potential values.

4. Conclusion

The association process between TiO₂ nanoparticles and alginate is found here mainly driven by an important gain of entropy due to the release of alginate counter-ions and water

molecules. Our results also suggest that the change of binding enthalpy, via electrostatic interactions, is favorable for the binding process and that this thermodynamic value is independent of concentration and mixing order. The mixing order is nevertheless found to play a key role on the reaction stoichiometry and for the molar charge ratio needed to fully saturate the binding sites available for complexation. This is due to different mechanisms of association (charge neutralization when TiO₂ is added to alginate, bridging when alginate is added to TiO₂). ITC measurements allows to determine and explicitly quantify important thermodynamic parameters (ΔH_b , K_b , ΔG and ΔS) and to propose, when associated with light scattering techniques, different mechanisms of interactions depending on the mixing order between engineered nanoparticles and natural organic matter. It should be noted that thermodynamic properties of adsorption could also be dependent on the particle size and type as well as surface site distribution.

Acknowledgments

The authors are grateful to the financial support received from the Swiss National Foundation (200020_152847 and 200021_135240). The work leading to these results also received funding from the European Union Seventh Framework Programme (FP7/2007-20013) under agreement no NMP4-LA-2013-310451. L.V. also thanks the CNPq (Conselho Nacional de Desenvolvimento Científico e Tecnológico) in Brazil for postdoctoral fellowship.

References

- Arnaud, A. and Bouteiller, L. (2004) Isothermal titration calorimetry of supramolecular polymers. *Langmuir* 20(16), 6858-6863.
- Auffan, M., Rose, J., Bottero, J.-Y., Lowry, G.V., Jolivet, J.-P. and Wiesner, M.R. (2009) Towards a definition of inorganic nanoparticles from an environmental, health and safety perspective. *Nature Nanotechnology* 4(10), 634-641.
- Baalousha, M. (2009) Aggregation and disaggregation of iron oxide nanoparticles: Influence of particle concentration, pH and natural organic matter. *Science of the Total Environment* 407(6), 2093-2101.
- Batley, G.E., Kirby, J.K. and McLaughlin, M.J. (2013) Fate and risks of nanomaterials in aquatic and terrestrial environments. *Accounts of Chemical Research* 46(3), 854-862.
- Belen Romanello, M. and Fidalgo de Cortalezzi, M.M. (2013) An experimental study on the aggregation of TiO₂ nanoparticles under environmentally relevant conditions. *Water Research* 47(12), 3887-3898.
- Bernhardt, H., Hoyer, O., Schell, H. and Lusse, B. (1985) Reaction-mechanisms involved In the influence of algogenic organic-matter on flocculation. *Zeitschrift Fur Wasser Und Abwasser Forschung-Journal for Water and Wastewater Research* 18(1), 18-30.
- Brinatti, C., Mello, L.B. and Loh, W. (2014) Thermodynamic Study of the Micellization of Zwitterionic Surfactants and Their Interaction with Polymers in Water by Isothermal Titration Calorimetry. *Langmuir* 30(21), 6002-6010.

Buffle, J., Wilkinson, K.J., Stoll, S., Filella, M. and Zhang, J.W. (1998) A generalized description of aquatic colloidal interactions: The three-colloidal component approach. *Environmental Science & Technology* 32(19), 2887-2899.

Carnal, F. and Stoll, S. (2011) Adsorption of Weak Polyelectrolytes on Charged Nanoparticles. Impact of Salt Valency, pH, and Nanoparticle Charge Density. Monte Carlo Simulations. *Journal of Physical Chemistry B* 115(42), 12007-12018.

Cedervall, T., Lynch, I., Lindman, S., Berggard, T., Thulin, E., Nilsson, H., Dawson, K.A. and Linse, S. (2007) Understanding the nanoparticle-protein corona using methods to quantify exchange rates and affinities of proteins for nanoparticles. *Proceedings of the National Academy of Sciences of the United States of America* 104(7), 2050-2055.

Chae, S.-R., Xiao, Y., Lin, S., Noeiaghahi, T., Kim, J.-O. and Wiesner, M.R. (2012) Effects of humic acid and electrolytes on photocatalytic reactivity and transport of carbon nanoparticle aggregates in water. *Water Research* 46(13), 4053-4062.

Chakraborti, S., Chatterjee, T., Joshi, P., Poddar, A., Bhattacharyya, B., Singh, S.P., Gupta, V. and Chakrabarti, P. (2010) Structure and Activity of Lysozyme on Binding to ZnO Nanoparticles. *Langmuir* 26(5), 3506-3513.

Chatterjee, T., Chakraborti, S., Joshi, P., Singh, S.P., Gupta, V. and Chakrabarti, P. (2010) The effect of zinc oxide nanoparticles on the structure of the periplasmic domain of the *Vibrio cholerae* ToxR protein. *Febs Journal* 277(20), 4184-4194.

Chen, X. and Mao, S.S. (2007) Titanium dioxide nanomaterials: Synthesis, properties, modifications, and applications. *Chemical Reviews* 107(7), 2891-2959.

Chiappisi, L., Hoffmann, I. and Gradzielski, M. (2013) Complexes of oppositely charged polyelectrolytes and surfactants - recent developments in the field of biologically derived polyelectrolytes. *Soft Matter* 9(15), 3896-3909.

Christian, P., Von der Kammer, F., Baalousha, M. and Hofmann, T. (2008) Nanoparticles: structure, properties, preparation and behaviour in environmental media. *Ecotoxicology* 17(5), 326-343.

Courtois, J. and Berret, J.F. (2010) Probing Oppositely Charged Surfactant and Copolymer Interactions by Isothermal Titration Microcalorimetry. *Langmuir* 26(14), 11750-11758.

Cozzoli, P.D., Comparelli, R., Fanizza, E., Curri, M.L. and Agostiano, A. (2003) Photocatalytic activity of organic-capped anatase TiO₂ nanocrystals in homogeneous organic solutions. *Materials Science & Engineering C-Biomimetic and Supramolecular Systems* 23(6-8), 707-713.

De, M., You, C.-C., Srivastava, S. and Rotello, V.M. (2007) Biomimetic interactions of proteins with functionalized nanoparticles: A thermodynamic study. *Journal of the American Chemical Society* 129(35), 10747-10753.

Domingos, R.F., Tufenkji, N. and Wilkinson, K.J. (2009) Aggregation of titanium dioxide nanoparticles: role of a fulvic acid. *Environmental Science & Technology* 43(5), 1282-1286.

Doyle, M.L. (1997) Characterization of binding interactions by isothermal titration calorimetry. *Current Opinion in Biotechnology* 8(1), 31-35.

Engel, A., Thoms, S., Riebesell, U., Rochelle-Newall, E. and Zondervan, I. (2004) Polysaccharide aggregation as a potential sink of marine dissolved organic carbon. *Nature* 428(6986), 929-932.

Erhayem, M. and Sohn, M. (2014) Stability studies for titanium dioxide nanoparticles upon adsorption of Suwannee River humic and fulvic acids and natural organic matter. *Science of the Total Environment* 468-469(0), 249-257.

Gallego-Urrea, J.A., Perez Holmberg, J. and Hasselov, M. (2014) Influence of different types of natural organic matter on titania nanoparticle stability: effects of counter ion concentration and pH. *Environmental Science: Nano* 1(2), 181-189.

Gombotz, W.R. and Wee, S.F. (1998) Protein release from alginate matrices. *Advanced Drug Delivery Reviews* 31(3), 267-285.

Gottschalk, F., Sonderer, T., Scholz, R.W. and Nowack, B. (2009) Modeled Environmental Concentrations of Engineered Nanomaterials (TiO₂, ZnO, Ag, CNT, Fullerenes) for Different Regions. *Environmental Science & Technology* 43(24), 9216-9222.

Gratzel, M. (2004) Conversion of sunlight to electric power by nanocrystalline dye-sensitized solar cells (vol 164, pg 3, 2004). *Journal of Photochemistry and Photobiology a-Chemistry* 168(3), 235-235.

Gregor, J.E., Fenton, E., Brokenshire, G., vandenBrink, P. and Osullivan, B. (1996) Interactions of calcium and aluminium ions with alginate. *Water Research* 30(6), 1319-1324.

Handy, R.D., Owen, R. and Valsami-Jones, E. (2008) The ecotoxicology of nanoparticles and nanomaterials: current status, knowledge gaps, challenges, and future needs. *Ecotoxicology* 17(5), 315-325.

Helgerud, T., Gåserød, O., Fjæreide, T., Andersen, P. O. and Larsen, C. K. (2009) Food Stabilisers, Thickeners and Gelling Agents. Imeson, A. (ed), pp. 50-72, Wiley-Blackwell, Oxford, UK.

Hendren, C.O., Mesnard, X., Droege, J. and Wiesner, M.R. (2011) Estimating production data for five engineered nanomaterials as a basis for exposure assessment. *Environmental Science & Technology* 45(7), 2562-2569.

Hyung, H., Fortner, J.D., Hughes, J.B. and Kim, J.-H. (2007) Natural organic matter stabilizes carbon nanotubes in the aqueous phase. *Environmental Science & Technology* 41(1), 179-184.

Jelesarov, I. and Bosshard, H.R. (1999) Isothermal titration calorimetry and differential scanning calorimetry as complementary tools to investigate the energetics of biomolecular recognition. *Journal of Molecular Recognition* 12(1), 3-18.

Jimin, X., Deli, J., Min, C., Di, L., Jianjun, Z., Xiaomeng, L. and Changhao, Y. (2010) Preparation and characterization of monodisperse Ce-doped TiO₂ microspheres with visible light photocatalytic activity. *Colloids and Surfaces A: Physicochemical and Engineering Aspects* 372(1-3).

Joshi, H., Shirude, P.S., Bansal, V., Ganesh, K.N. and Sastry, M. (2004) Isothermal titration calorimetry studies on the binding of amino acids to gold nanoparticles. *Journal of Physical Chemistry B* 108(31), 11535-11540.

Kamiya, M., Torigoe, H., Shindo, H. and Sarai, A. (1996) Temperature dependence and sequence specificity of DNA triplex formation: An analysis using isothermal titration calorimetry. *Journal of the American Chemical Society* 118(19), 4532-4538.

Khan, R. and Dhayal, M. (2008) Electrochemical studies of novel chitosan/TiO₂ bioactive electrode for biosensing application. *Electrochemistry Communications* 10(2), 263-267.

Kim, W., Yamasaki, Y., Jang, W.-D. and Kataoka, K. (2010) Thermodynamics of DNA condensation induced by poly(ethylene glycol)-block-polylysine through polyion complex micelle formation. *Biomacromolecules* 11(5), 1180-1186.

Klaine, S.J., Alvarez, P.J.J., Batley, G.E., Fernandes, T.F., Handy, R.D., Lyon, D.Y., Mahendra, S., McLaughlin, M.J. and Lead, J.R. (2008) Nanomaterials in the environment: Behavior, fate, bioavailability, and effects. *Environmental Toxicology and Chemistry* 27(9), 1825-1851.

Kominami, H., Itonaga, M., Shinonaga, A., Kagawa, K., Konishi, S. and Kera, Y. (2000) *Studies in Surface Science and Catalysis*. E. Gaigneaux, D.D., P. Grange, P. A. Jacobs, J. A. Martens, P. Ruiz, and Poncelet, G. (eds), pp. 1089-1096, Elsevier.

Ladbury, J.E. (2001) Isothermal titration calorimetry: application to structure-based drug design. *Thermochimica Acta* 380(2), 209-215.

Lee, K.Y. and Mooney, D.J. (2012) Alginate: Properties and biomedical applications. *Progress in Polymer Science* 37(1), 106-126.

Lin, S., Cheng, Y., Liu, J. and Wiesner, M.R. (2012) Polymeric coatings on silver nanoparticles hinder autoaggregation but enhance attachment to uncoated surfaces. *Langmuir* 28(9), 4178-4186.

Liu, X., Wazne, M., Han, Y., Christodoulatos, C. and Jasinkiewicz, K.L. (2010) Effects of natural organic matter on aggregation kinetics of boron nanoparticles in monovalent and divalent electrolytes. *Journal of Colloid and Interface Science* 348(1), 101-107.

Loosli, F., Le Coustumer, P. and Stoll, S. (2013) TiO₂ nanoparticles aggregation and disaggregation in presence of alginate and Suwannee River humic acids. pH and concentration effects on nanoparticle stability. *Water Research* 47(16), 6052-6063.

Loosli, F., Le Coustumer, P. and Stoll, S. (2014) Effect of natural organic matter on the disagglomeration of manufactured TiO₂ nanoparticles. *Environmental Science: Nano* 1, 154-160.

Louie, S.M., Tilton, R.D. and Lowry, G.V. (2013) Effects of Molecular Weight Distribution and Chemical Properties of Natural Organic Matter on Gold Nanoparticle Aggregation. *Environmental Science & Technology* 47(9), 4245-4254.

Lu, A.-H., Salabas, E.L. and Schueth, F. (2007) Magnetic nanoparticles: Synthesis, protection, functionalization, and application. *Angewandte Chemie-International Edition* 46(8), 1222-1244.

Luo, X.L., Morrin, A., Killard, A.J. and Smyth, M.R. (2006) Application of nanoparticles in electrochemical sensors and biosensors. *Electroanalysis* 18(4), 319-326.

Mahlfig, B., Bottcher, H., Rauch, K., Dieckmann, U., Nitsche, R. and Fritz, T. (2005) Optimized UV protecting coatings by combination of organic and inorganic UV absorbers. *Thin Solid Films* 485(1-2), 108-114.

Martin, M., Celi, L., Barberis, E., Violante, A., Kozak, L.M. and Huang, P.M. (2009) Effect of humic acid coating on arsenic adsorption on ferrihydrite-kaolinite mixed systems. *Canadian Journal of Soil Science* 89(4), 421-434.

Matulis, D., Rouzina, I. and Bloomfield, V.A. (2002) Thermodynamics of cationic lipid binding to DNA and DNA condensation: Roles of electrostatics and hydrophobicity. *Journal of the American Chemical Society* 124(25), 7331-7342.

Mohd Omar, F., Abdul Aziz, H. and Stoll, S. (2014) Aggregation and disaggregation of ZnO nanoparticles: Influence of pH and adsorption of Suwannee River humic acid. *Science of the Total Environment* 468-469(0), 195-201.

Palomino, D. and Stoll, S. (2013) Fulvic acids concentration and pH influence on the stability of hematite nanoparticles in aquatic systems. *Journal of Nanoparticle Research* 15(2), 1-8.

Piccinno, F., Gottschalk, F., Seeger, S. and Nowack, B. (2012) Industrial production quantities and uses of ten engineered nanomaterials in Europe and the world. *Journal of Nanoparticle Research* 14(9).

Ravi, V., Binz, J.M. and Rioux, R.M. (2013) Thermodynamic profiles at the solvated inorganic-organic interface: The case of gold-thiolate monolayers. *Nano Letters* 13(9), 4442-4448.

Sani-Kast, N., Scheringer, M., Slomberg, D., Labille, J., Praetorius, A., Ollivier, P. and Hungerbühler, K. (2015) Addressing the complexity of water chemistry in environmental fate modeling for engineered nanoparticles. *Science of the Total Environment*, In Press, doi:10.1016/j.scitotenv.2014.1012.1025.

Saude, N., Cheze-Lange, H., Beunard, D., Dhulster, P., Guillochon, D., Caze, A.M., Morcellet, M. and Junter, G.A. (2002) Alginate production by *Azotobacter vinelandii* in a membrane bioreactor. *Process Biochemistry* 38(2), 273-278.

Schmid, K. and Riediker, M. (2008) Use of nanoparticles in Swiss industry: A targeted survey. *Environmental Science & Technology* 42(7), 2253-2260.

Seitz, F., Bundschuh, M., Dabrunz, A., Bandow, N., Schaumann, G.E. and Schulz, R. (2012) Titanium dioxide nanoparticles detoxify pirimicarb under UV irradiation at ambient intensities. *Environmental Toxicology and Chemistry* 31(3), 518-523.

Shen, M.-H., Yin, Y.-G., Booth, A. and Liu, J.-F. (2015) Effects of molecular weight-dependent physicochemical heterogeneity of natural organic matter on the aggregation of fullerene nanoparticles in mono- and di-valent electrolyte solutions. *Water Research* 71(0), 11-20.

Sheng, G.-P., Xu, J., Luo, H.-W., Li, W.-W., Li, W.-H., Yu, H.-Q., Xie, Z., Wei, S.-Q. and Hu, F.-C. (2013) Thermodynamic analysis on the binding of heavy metals onto extracellular polymeric substances (EPS) of activated sludge. *Water Research* 47(2), 607-614.

Vitorazi, L., Ould-Moussa, N., Sekar, S., Fresnais, J., Loh, W., Chapel, J.P. and Berret, J.F. (2014) Evidence of a two-step process and pathway dependency in the thermodynamics of poly(diallyldimethylammonium chloride)/poly(sodium acrylate) complexation. *Soft Matter* 10(47), 9496-9505.

von Moos, N. and Slaveykova, V.I. (2014) Oxidative stress induced by inorganic nanoparticles in bacteria and aquatic microalgae - state of the art and knowledge gaps. *Nanotoxicology* 8(6), 605-630.

Weir, A., Westerhoff, P., Fabricius, L., Hristovski, K. and von Goetz, N. (2012) Titanium dioxide nanoparticles in food and personal care products. *Environmental Science & Technology* 46(4), 2242-2250.

Wells, M.L. (1998) Marine colloids - A neglected dimension. *Nature* 391(6667), 530-531.

Wilkinson, K.J., Balnois, E., Leppard, G.G. and Buffle, J. (1999) Characteristic features of the major components of freshwater colloidal organic matter revealed by transmission electron and atomic force microscopy. *Colloids and Surfaces a-Physicochemical and Engineering Aspects* 155(2-3), 287-310.

Wilkinson, K.J., Joz-Roland, A. and Buffle, J. (1997) Different roles of pedogenic fulvic acids and aquagenic biopolymers on colloid aggregation and stability in freshwaters. *Limnology and Oceanography* 42(8), 1714-1724.

Wongkalasin, P., Chavadej, S. and Sreethawong, T. (2011) Photocatalytic degradation of mixed azo dyes in aqueous wastewater using mesoporous-assembled TiO₂ nanocrystal synthesized by a modified sol-gel process. *Colloids and Surfaces a-Physicochemical and Engineering Aspects* 384(1-3), 519-528.

Yang, J., Zhao, J. and Fang, Y. (2008) Calorimetric studies of the interaction between sodium alginate and sodium dodecyl sulfate in dilute solutions at different pH values. *Carbohydrate Research* 343(4), 719-725.

Zhang, A.-P. and Sun, Y.-P. (2004) Photocatalytic killing effect of TiO₂ nanoparticles on Ls-174-t human colon carcinoma cells. *World Journal of Gastroenterology* 10(21), 3191-3193.

Zhang, W., Rattanadompol, U.s., Li, H. and Bouchard, D. (2013) Effects of humic and fulvic acids on aggregation of aqu/nC60 nanoparticles. *Water Research* 47(5), 1793-1802.

Zhang, Y., Chen, Y., Westerhoff, P. and Crittenden, J. (2009) Impact of natural organic matter and divalent cations on the stability of aqueous nanoparticles. *Water Research* 43(17), 4249-4257.

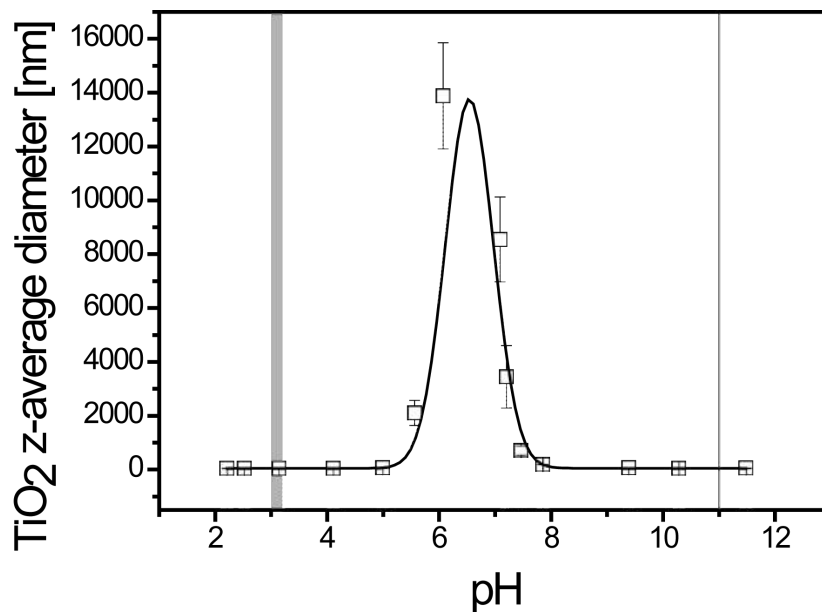


Fig. S1 - TiO₂ z-average diameter values as a function of pH. At pH 3.1 (large gray vertical line) the TiO₂ ENPs are dispersed with a z-average diameter value found equal to 47 ± 1 nm. At pH 11.0 (narrow gray line), the ENPs are also stable with diameter value equal to 53 ± 1 nm. $[\text{TiO}_2] = 50 \text{ mg L}^{-1}$ and $[\text{NaCl}] = 0.001 \text{ M}$.

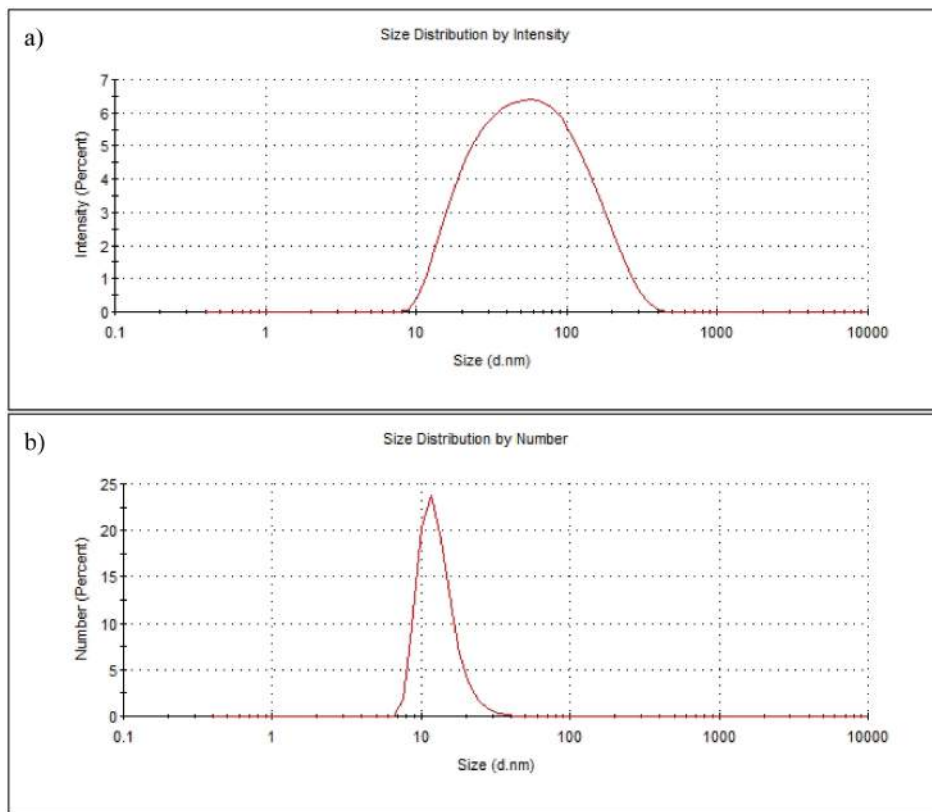


Fig. S2 - TiO₂ ENPs intensity and number size distribution at pH < pH_{PCN,ENPs}. [TiO₂] = 50 mg L⁻¹.

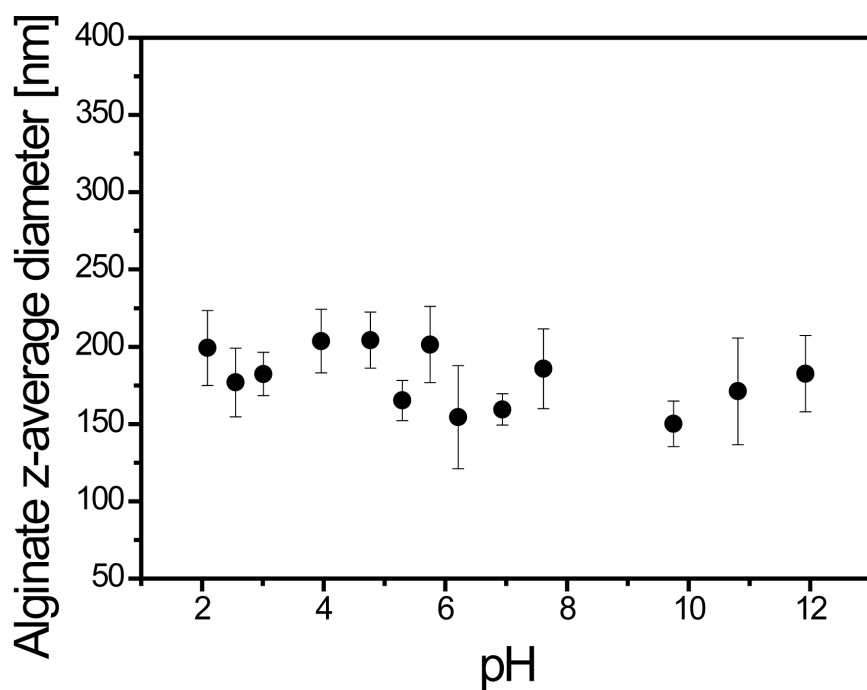


Fig. S3 - Alginate z-average diameter values as a function of pH. Alginate z-average diameter is constant with diameter value equal to 178 ± 21 nm. $[\text{Alginate}] = 100 \text{ mg L}^{-1}$.

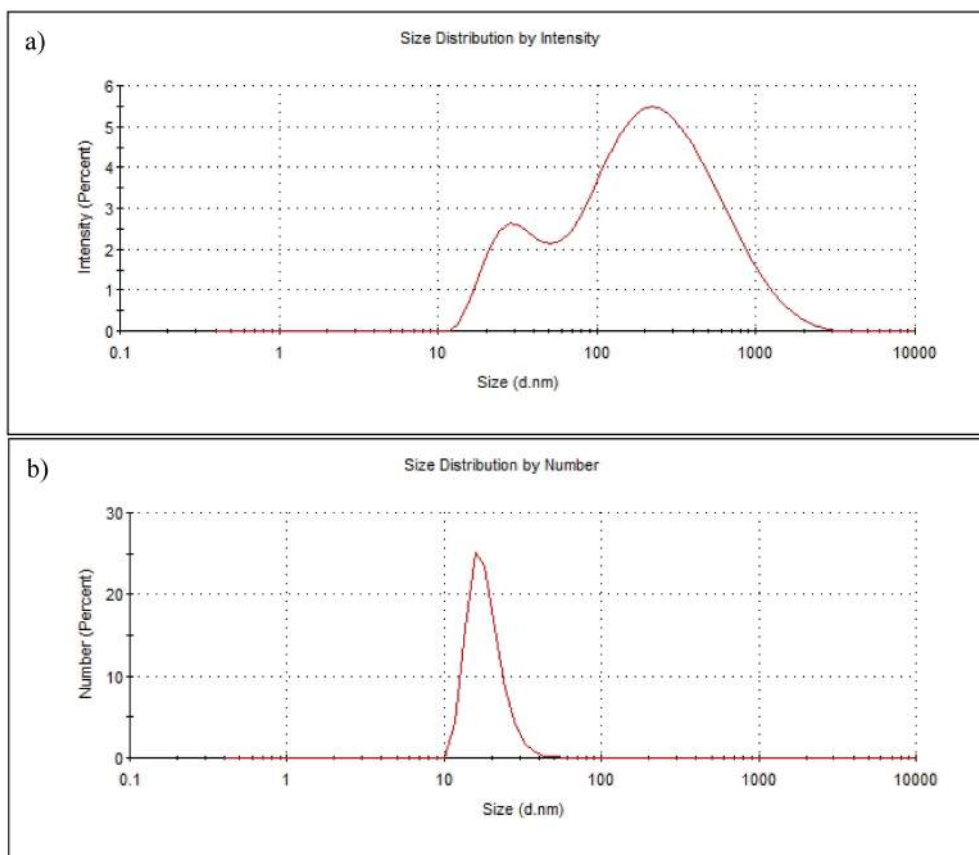


Fig. S4 - Alginate intensity and number size distribution at $\text{pH} < \text{pH}_{\text{PCN,ENPs}}$. $[\text{Alginate}] = 100 \text{ mg L}^{-1}$.

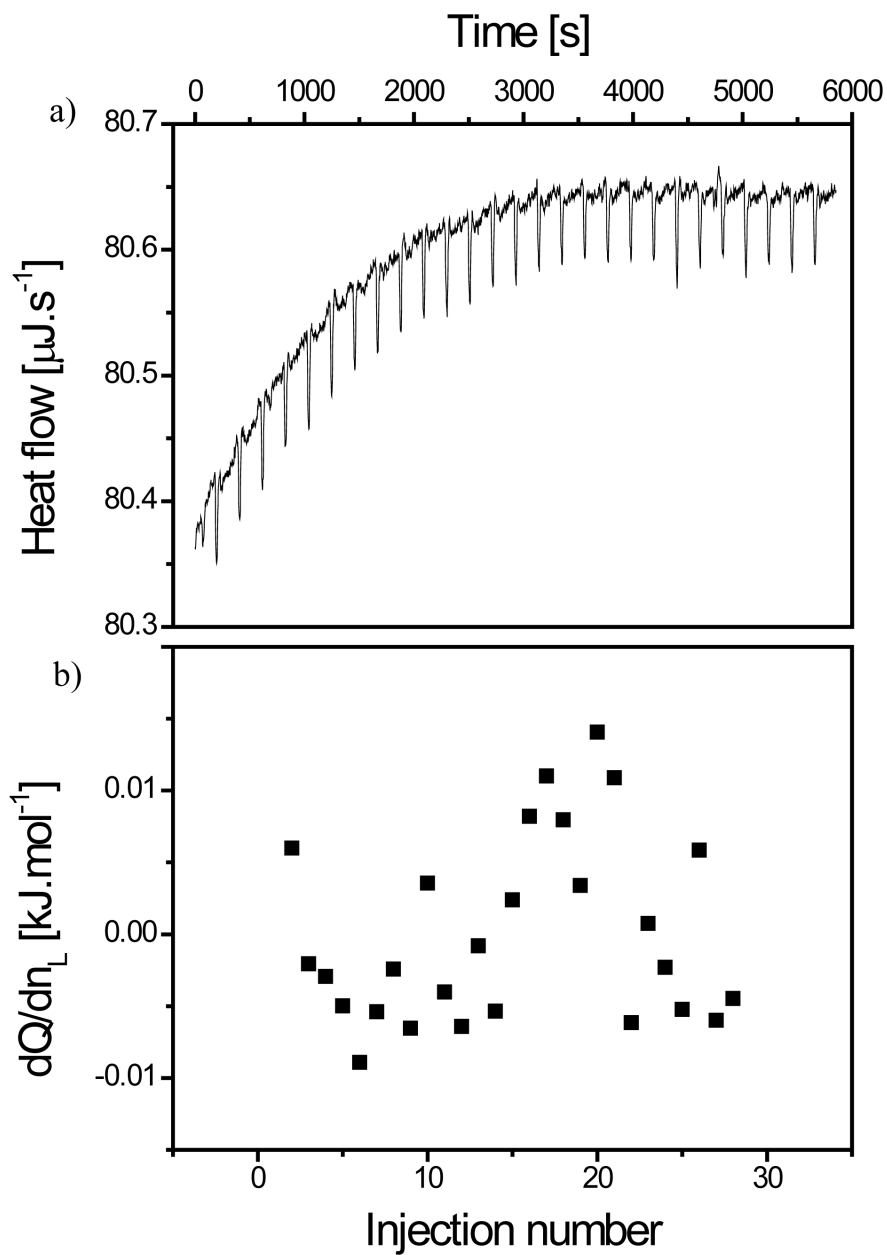


Fig. S5 - a) Real-time thermogram representing the heat exchange for a 2.5 mM alginate charge concentration titration in water at $\text{pH} < \text{pH}_{\text{PCN,TiO}_2}$. b) Corresponding interaction binding enthalpy as a function of injection number. Only dilution effect is observed.

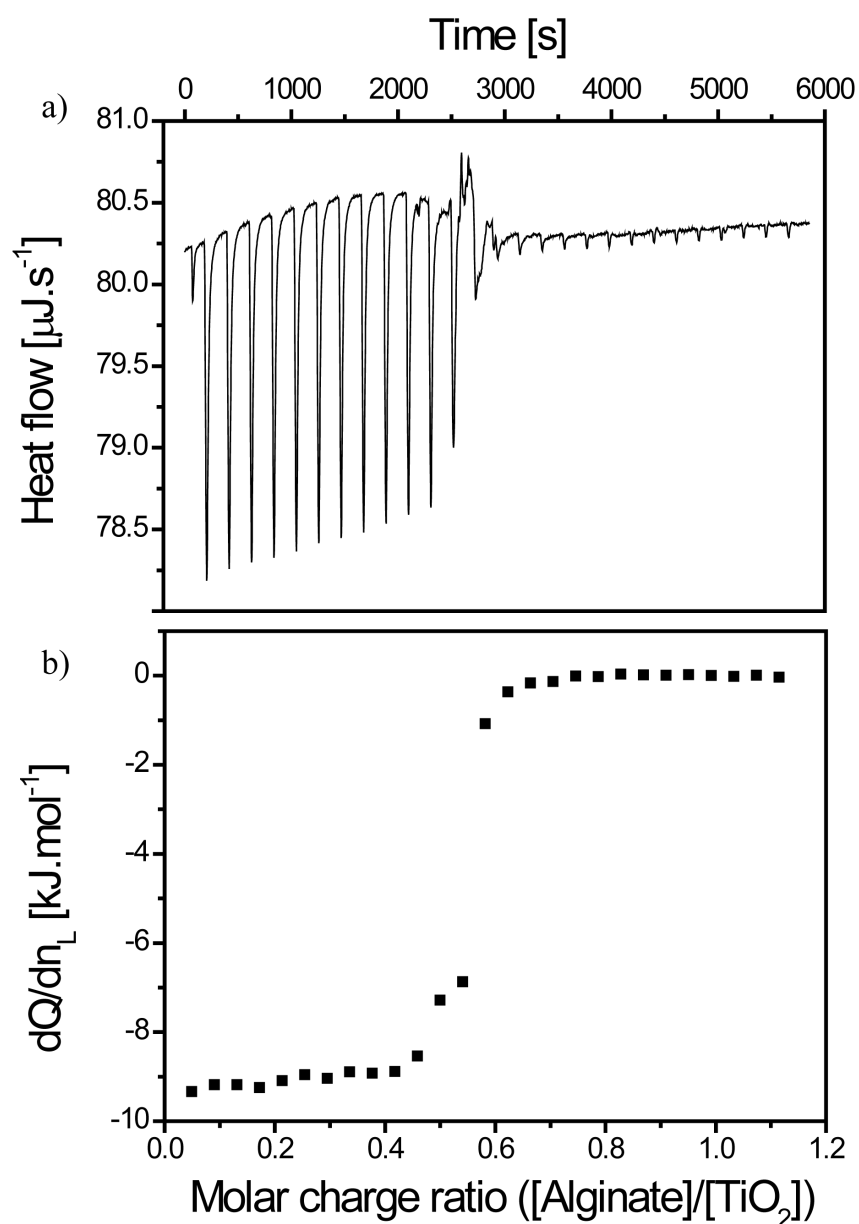


Fig. S6 - a) Real-time thermogram for TiO_2 0.14 g L^{-1} titration with alginate 0.7 mM at $\text{pH} < \text{pH}_{\text{PCN},\text{TiO}_2}$ at 298.15 K . Negative peaks indicate an exothermic reaction. After about fifteen injections sites saturation occurs and only dilution effect is observed (small negative peaks). b) Corresponding integrated heat data as a function of molar charge ratio.

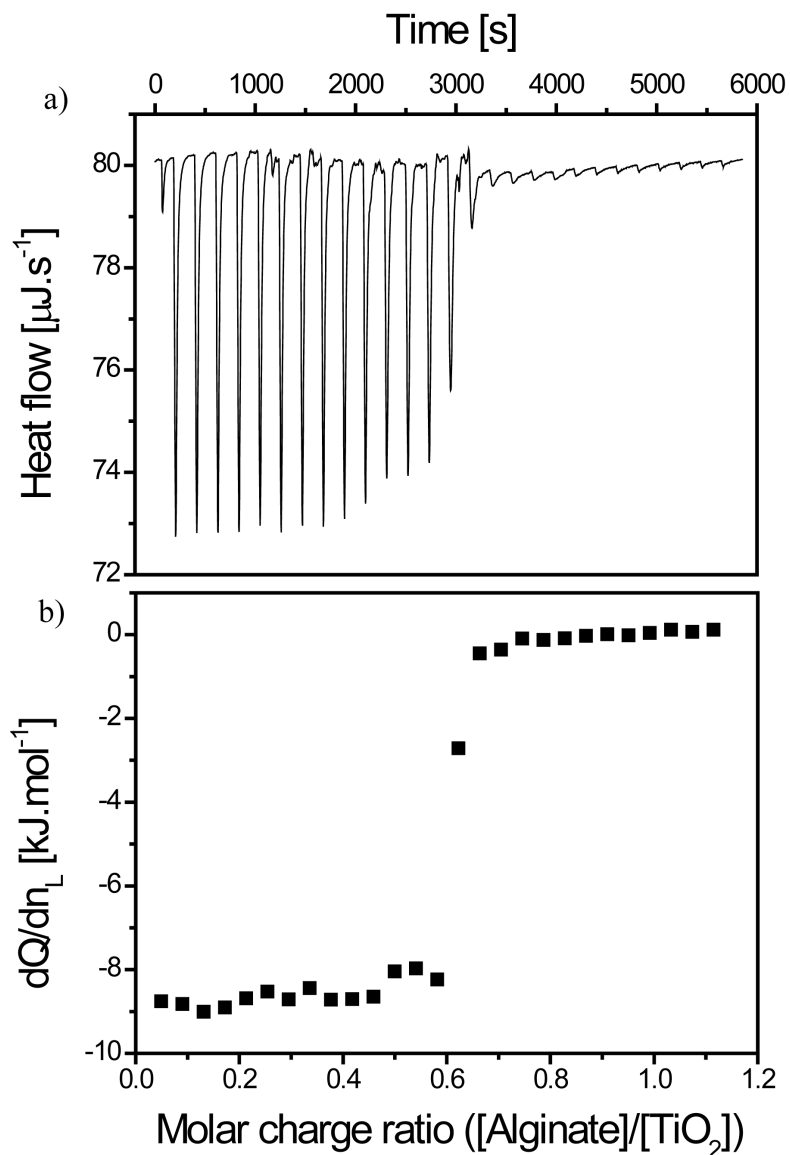


Fig. S7 - a) Real-time thermogram for TiO_2 0.5 g L^{-1} titration with alginate 2.5 mM at $\text{pH} < \text{pH}_{\text{PCN},\text{TiO}_2}$ at 298.15 K . Negative peaks indicate an exothermic reaction. After about fifteen injections sites saturation occurs and only dilution effect is observed (small negative peaks). b) Corresponding integrated heat data as a function of molar charge ratio.

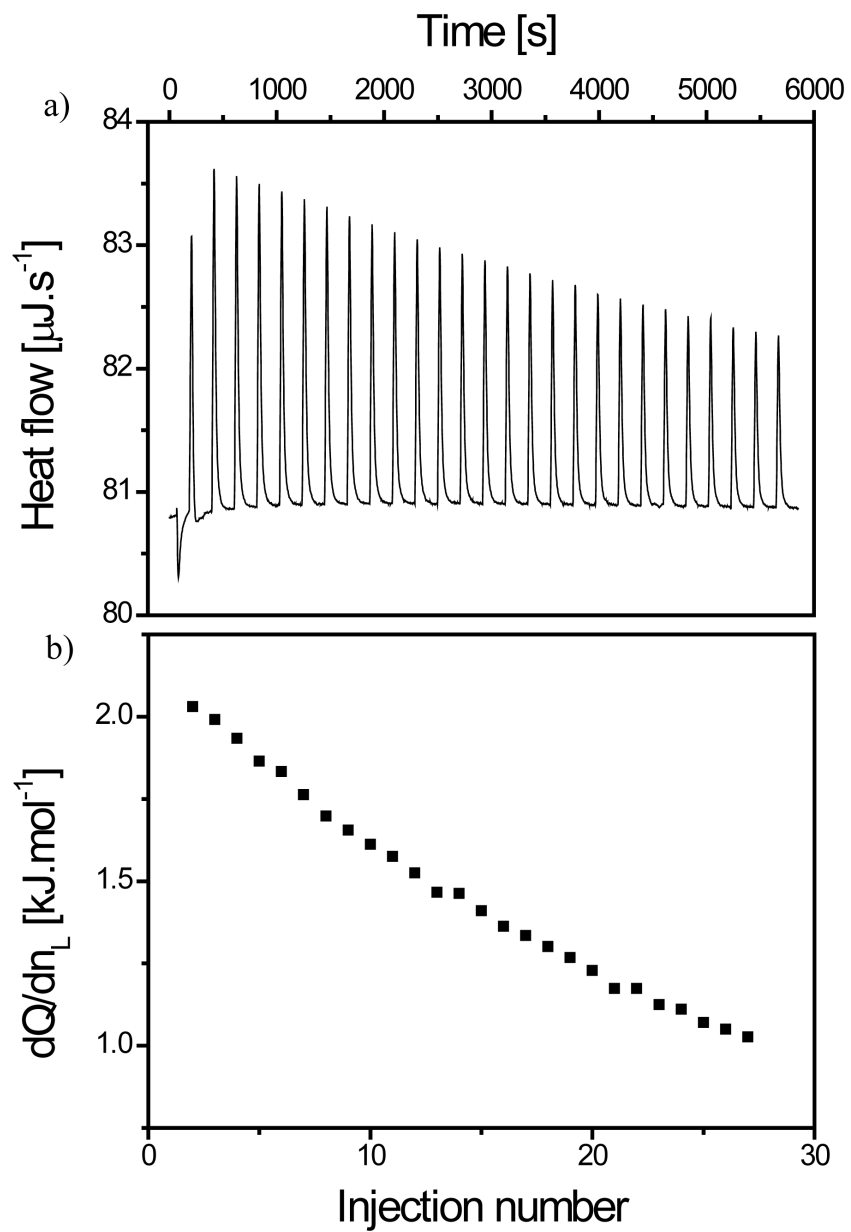


Fig. S8 - a) Real-time thermogram and b) the corresponding integrated heat data as a function of injection number for a 5 g L^{-1} TiO_2 dispersion titration in water at $\text{pH} < \text{pH}_{\text{PCN},\text{TiO}_2}$ and at 298.15 K . Dilution effect is observed. The dilution of the TiO_2 ENPs in water is an endothermic process.

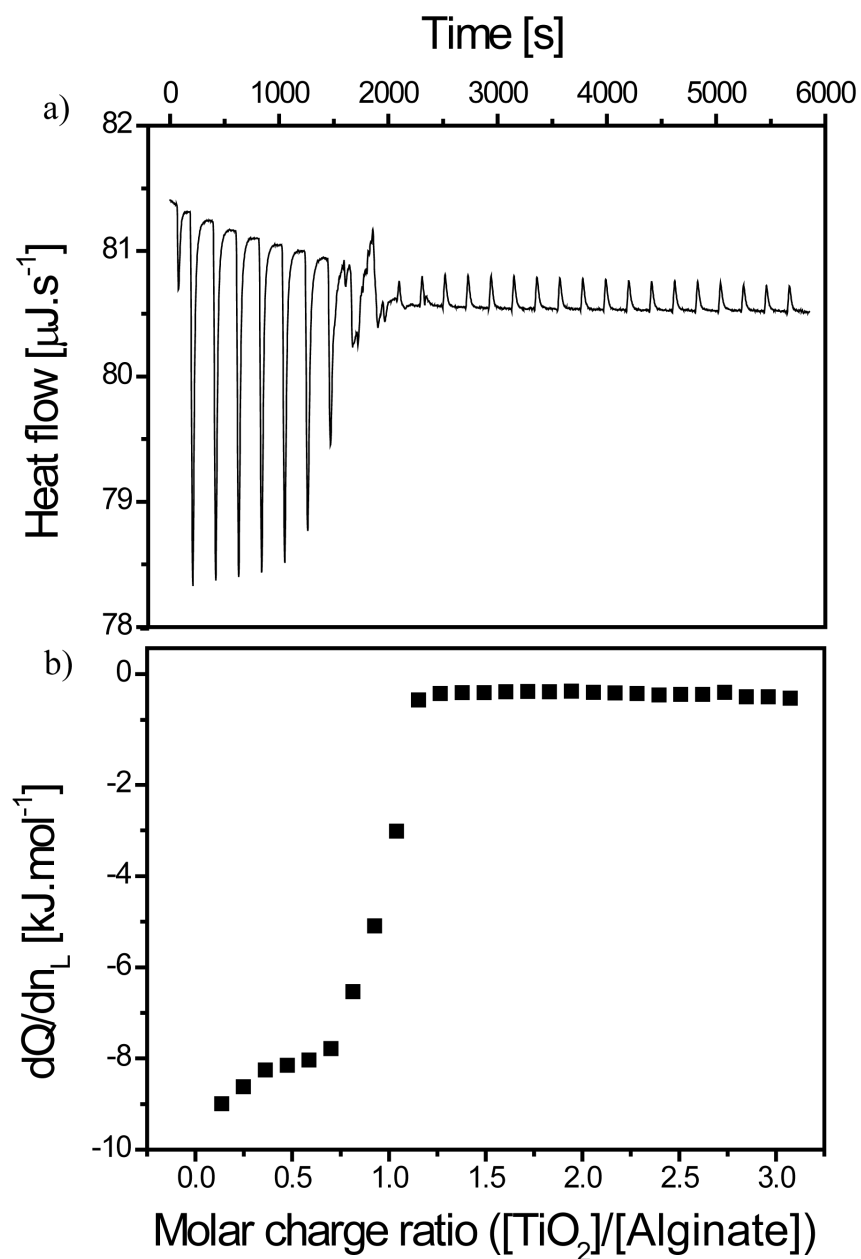


Fig. S9 - a) Real-time thermogram for alginate 0.07 mM titration with TiO_2 1.4 g L^{-1} at $\text{pH} < \text{pH}_{\text{PCN},\text{TiO}_2}$ and at 298.15 K. Negative peaks indicate an exothermic reaction. After about ten injections sites saturation occurs and only dilution effect is observed (small positive peaks). b) Corresponding integrated heat data as a function of molar charge ratio.

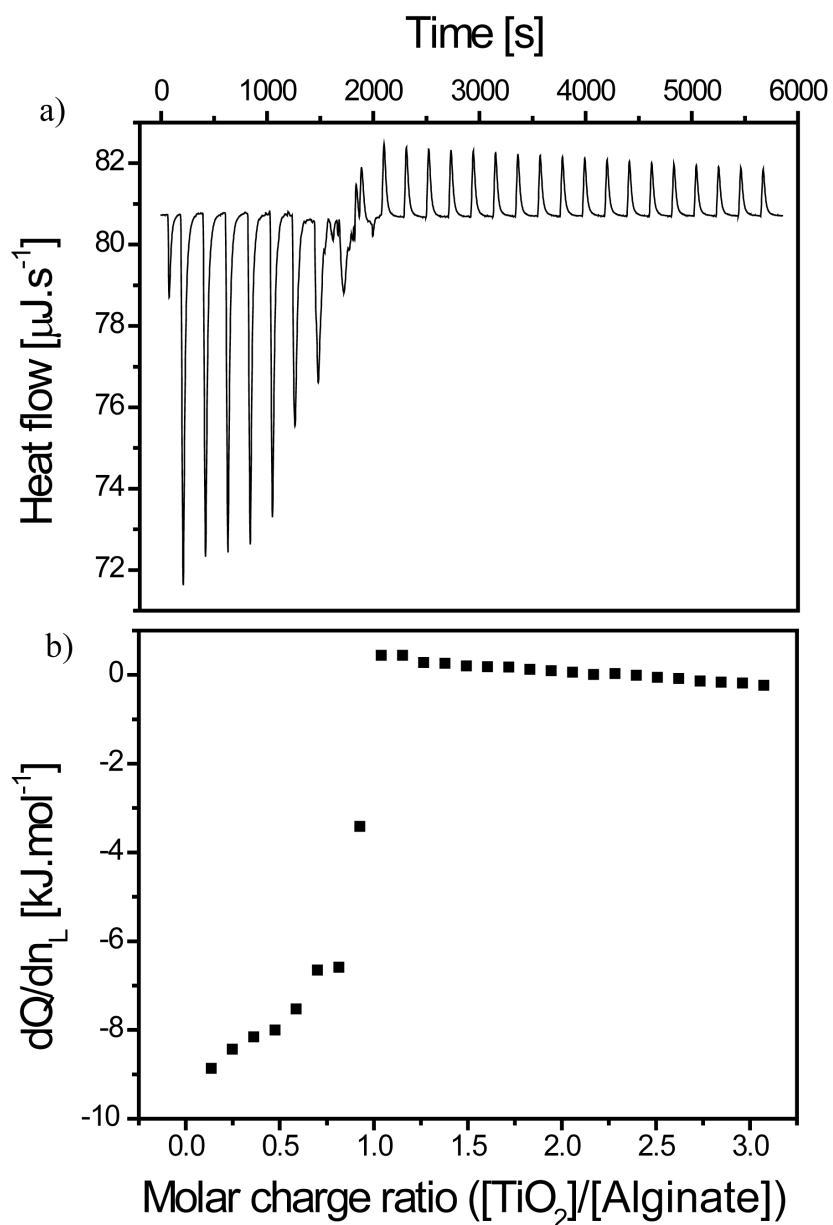


Fig. S10 - a) Real-time thermogram for alginate 0.25 mM titration with TiO_2 5 g L^{-1} at $\text{pH} < \text{pH}_{\text{PCN},\text{TiO}_2}$ and at 298.15 K. Negative peaks indicate an exothermic reaction. After about ten injections sites saturation occurs and only dilution effect is observed (small positive peaks). b) Corresponding integrated heat data as a function of molar charge ratio

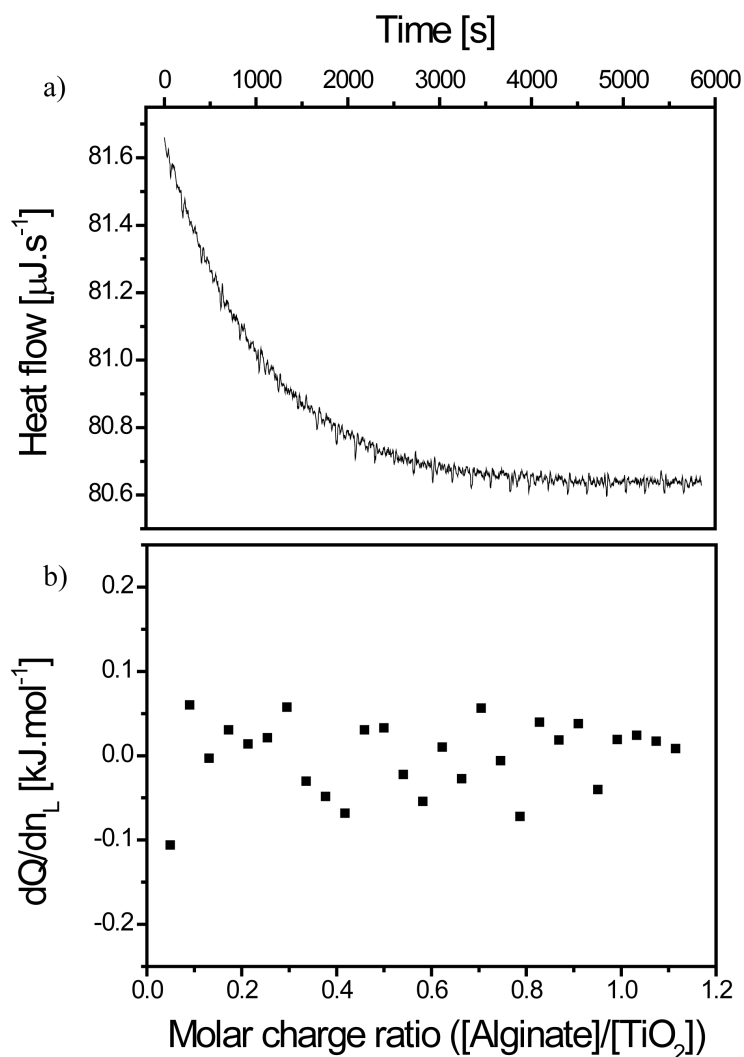


Fig. S11 - a) Real-time thermogram representing the heat exchange for a 0.1 g L^{-1} TiO_2 titration with a 0.5 mM charge concentration alginate at pH 11.0. b) Corresponding integrated heat exchange data as a function of alginate over TiO_2 . No interaction is observed in agreement with electrostatic repulsions between the negatively charged compounds (Fig. 2).